EUROFUSION WPRM-CP(16) 15561

Y Wang et al.

Accuracy improvement studies for Remote Maintenance Manipulators

Preprint of Paper to be submitted for publication in Proceedings of 29th Symposium on Fusion Technology (SOFT 2016)

This work has been carried out within the framework of the EUROfusion Consortium and has received funding from the Euratom research and training programme 2014-2018 under grant agreement No 633053. The views and opinions expressed herein do not necessarily reflect those of the European Commission.

Accuracy improvement studies for remote maintenance manipulators

Yongbo Wang[a,*], Huapeng Wu[a], Heikki Handroos[a], Ming Li[a], Bingyan Mao[a], Jing Wu[a], Antony Loving[b], Matti Coleman[c], Oliver Crofts[b], Jonathan Keep[b]

[a]*Laboratory of Intelligent Machines, Lappeenranta University of Technology, FIN-53851 Lappeenranta,Finland*
[b]*EUROfusion Consortium, JET, Culham Science Centre, Abingdon, OX14 3DB, UK*
[c]*EUROfusion Consortium, Boltzmannstr.2, Garching 85748,Germany*

For ITER or the future DEMO remote maintenance system (WPRM), several types of special tailored automatic manipulators are needed for vacuum vessel (VV) component transportation, inspection, and removal from and replacement to the VV wall. Due to the extreme work conditions such as big size, big payload and high environment temperature, both the static and dynamic error sources should be considered when design a controller. In this paper, the accuracy improvement issues regarding the static and dynamic error sources are taken into account. The paper proposed a plane constraint calibration method for static error calibration, whilst the dynamic errors are calibrated using a linear inverse dynamic error model. Differential Evolution global optimization method is used to generate optimal excitation trajectories, and to identify the static and dynamic parameter errors. A 6-DOF (degrees of freedom) commercial industrial serial robot was employed to carry out the corresponding simulation and experimental studies. This paper mainly focus on the general case studies, the results found in this research would be extrapolated to support the ITER or the future DEMO remote handling systems.

Keywords: DEMO; remote handling; kinematic calibration; dynamic calibration; plane constraint

1. Introduction

The remote handling of big size and massive component in a challenging environment plays a crucial role in the construction of future fusion reactors. For the EU DEMO blanket remote handling systems (see Figure 1), the required positioning tolerance is expected to be tens of millimeters. However, due to big size and massive weight of the manipulator and its lifting component, the unknown errors originated from geometric dimensions, dynamic motion, as well as joint and link deformations will become considerably large, in the worst case it would be up to several hundred millimeters. To satisfy the accuracy requirement, both geometric and dynamic errors should be calibrated and then compensated in controller.

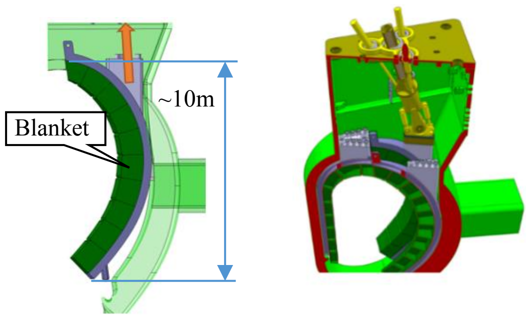

Fig. 1. Remote handling of blanket.

During the past several decades, a great deal of kinematic calibration methods have been proposed. Essentially, all kinematic calibration methods can be regarded as closed-loop methods if the endpoint measurement system is considered to form a joint [1]. Practically, the endpoint can be constrained by a point fixture [2], a virtual line [3], or multiple planes [4, 5]. For plane constraint method, one approach is based on the use of plane equation and another is on calculating plane normal coordinates. Unlike the previous plane-constraint methods, this paper show that it is also possible to carry out kinematic calibration without calculating plane equation or normal coordinates. The proposed method is based on a common mathematical truth that four points are coplanar if and only if the volume of a tetrahedron defined by these four points is zero.

Dynamic calibration involves experimental identification of dynamic parameters such as link masses, joint friction, and the moment inertial. In general, an inverse dynamic model has to be established, and then the dynamic parameters are grouped as base parameters according to the rules defined by Khalil et al [6]. In order to identify the base parameters, optimal excitation trajectories are indispensable. In the literature, periodic excitation trajectories based on Fourier series are the most commonly used ones [7]. In this paper, a symbolic linear dynamic identification model was built up. Fourier series excitation trajectories are generated by minimizing condition number of the observation matrix, and then SimMechanics was used to simulate the real robot to get joint torques for dynamic parameter identification purpose. A global optimization method, i.e. Differential Evolution (DE) algorithm [8], is utilized in three different objective functions in order to identify geometrical errors, dynamic errors, and generate Fourier series excitation trajectories respectively.

2. Kinematic modeling and identification

2.1 The principal of the proposed method

The idea behand this method is to calculate the volume of a parallelepiped (V_p) defined by three vectors given four points: $A(x_1, y_1, z_1)$, $B(x_2, y_2, z_2)$, $C(x_3, y_3, z_3)$, $D(x_4, y_4, z_4)$, as shown in figure 2. The volume of the

* Corresponding author's email: *yongbo.wang@lut.fi*

tetrahedron (V_t) can be obtained by calculating the scalar triple product of the three vectors as seen in equation (1).

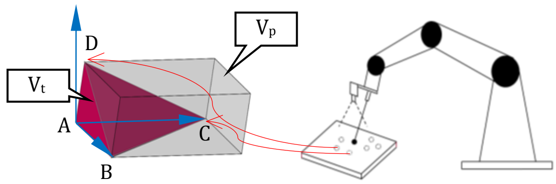

Fig. 2. Principal of the proposed method.

$$V_p = \overrightarrow{AD} \cdot \left(\overrightarrow{AB} \times \overrightarrow{AC}\right), \qquad V_t = \frac{1}{6} V_p \tag{1}$$

2.2 Kinematic identification model

The forward kinematics of a serial manipulator can be obtained using the commonly used Denavit-Hartenberg conventions [6].

$$ {}^{B}T_E = \prod_{i=1}^{n} {}^{i-1}A_i , \quad {}^{B}T_E' = \prod_{i=1}^{n} {}^{i-1}A_i' \tag{2}$$

$$ {}^{i\text{-}1}\mathrm{A}_i = \begin{bmatrix} c\theta_i & -s\theta_i & 0 & d_i \\ c\alpha_i \cdot s\theta_i & c\alpha_i \cdot c\theta_i & -s\alpha_i & -r_i \cdot s\alpha_i \\ s\alpha_i \cdot s\theta_i & s\alpha_i \cdot c\theta_i & c\alpha_i & r_i \cdot c\alpha_i \\ 0 & 0 & 0 & 1 \end{bmatrix} \tag{3}$$

$$ {}^{i\text{-}1}\mathrm{A}_i' = \begin{bmatrix} c\theta_i & -s\theta_i & 0 & d_i' \\ c\alpha_i' \cdot s\theta_i & c\alpha_i' \cdot c\theta_i & -s\alpha_i' & -r_i' \cdot s\alpha_i' \\ s\alpha_i' \cdot s\theta_i & s\alpha_i' \cdot c\theta_i & c\alpha_i' & r_i' \cdot c\alpha_i' \\ 0 & 0 & 0 & 1 \end{bmatrix} \tag{4}$$

where ${}^{B}T_E$ and ${}^{B}T_B'$ denote the nominal and the predicted position and orientation of the endpoint frame {E} with respect to the robot base frame {B}; ${}^{i-1}A_i$ denotes the homogeneous transformation matrix between two successive joints; $s\alpha_i'$ represents $\sin(\alpha_i + \delta\alpha_i)$, and $\delta\alpha_i$ represents a small unknown parameter errors, the same rules are also applied to the other two geometric parameters d_i' and r_i'.

For this method, the only thing need to know is the joint sensor readings and the distance between the end-effector and a smooth planar surface. By using these measured data, a predicted point on the planar surface can be calculated according to equations (2) and (4). Repeating this process for different robot configurations and on different plane locations, an identification cost function can be established as seen in equation (5). And a global optimization algorithm, Differential Evolution algorithm, was employed to identify the unknown parameters.

$$\min_{(\delta\mathbf{\alpha},\delta\mathbf{d},\delta\mathbf{r})} \sum_{i}^{n}\sum_{j}^{m} abs(V_t^{i,j}), \tag{5}$$

where $V_t^{i,j}$ is the predicted tetrahedron volume including unknown variables $\delta\mathbf{\alpha}$, $\delta\mathbf{d}$ and $\delta\mathbf{r}$ for the *i-th* plane and *j-th*.

It should be noted that the plane can be fixed in any location of the robot workspace, and the robot can be calibrated without calibrating the transformation from plane coordinate system with respect to robot base coordinate system. This makes robot calibration very easy and convenient to implement on the site.

3. Dynamic modeling and identification

3.1 Dynamic identification model

This paper employs inverse dynamic model and least squares estimation method to estimate dynamic parameters. The dynamic model can be derived using the Euler-Lagrange formulation [6] and written as:

$$\boldsymbol{\tau} = \mathbf{M}(q)\ddot{\mathbf{q}} + \mathbf{B}\dot{\mathbf{q}}\dot{\mathbf{q}} + \mathbf{C}\dot{\mathbf{q}}^2 + \mathbf{Q} + \tau_f \tag{6}$$

where **M** is inertial matrix, **B** matrix containing the elements of Coriolis forces, **C** matrix containing the elements of centrifugal forces, $\mathbf{Q}=[Q_1 \ldots Q_n]^T$ is gravity forces vector,

$$\dot{\mathbf{q}}\dot{\mathbf{q}} = \left[\dot{q}_1\dot{q}_2 \quad \cdots \quad \dot{q}_1\dot{q}_n \quad \dot{q}_2\dot{q}_3 \quad \cdots \quad \dot{q}_{n-1}\dot{q}_n\right]^T \tag{7}$$

$$\dot{\mathbf{q}}^2 = \left[\dot{q}_1^2 \quad \cdots \quad \dot{q}_n^2\right]^T, \quad \tau_f = f_v\,\dot{q} + f_c\,\mathrm{sgn}(\dot{q}) \; . \tag{8}$$

A linearly parametrized form of equation (6) is:

$$\boldsymbol{\tau} = \mathbf{Y}_s(q,\dot{q},\ddot{q})\chi_s \tag{9}$$

where $\mathbf{Y}_s(q,\dot{q},\ddot{q}) \in \Re^{n\times N_s}$ is observation matrix, $\chi_s \in \Re^{N_s\times 1}$ is a vector of 13 standard parameters including six components of the inertia matrix (XX_j, XY_j, XZ_j, YY_j, YZ_j, ZZ_j), three components of the first moments (MX_j, MY_j, MZ_j), the mass (M_j) of link j, the rotor and gears inertial moment (Ia_j), and viscous and Coulomb friction coefficients (fv_j, fv_j). For a rigid robots with *n* joints, the number of standard parameters can also be further reduced by eliminating dependent parameters or regrouping with others, finally a dynamic equation with minimal identifiable parameters can be obtained as:

$$\boldsymbol{\tau} = \mathbf{Y}(q,\dot{q},\ddot{q})\chi_b \tag{10}$$

where $\mathbf{Y}(q,\dot{q},\ddot{q}) \in \Re^{n\times N_b}$ is a subset of the independent columns of $\mathbf{Y}_s$ and $\chi_b \in \Re^{N_b\times 1}$ are the base parameters [9].

3.2 Trajectory parametrization and optimization

To identify the base dynamic parameters, an excitation reference trajectory must be generated to persistently excite a given system. In this work, a periodic Fourier series trajectory was employed. The trajectory of each joint can be expressed as a sum of N harmonic sine and cosine functions [10]. The *i-th* joint position, velocity, and acceleration can be written as:

$$q_i(t) = \sum_{l=1}^{N} \frac{a_l}{\omega_f l}\sin(\omega_f lt) - \frac{b_l}{\omega_f l}\cos(\omega_f lt) \tag{11}$$

$$\dot{q}_i(t) = \sum_{l=1}^{N} a_l\cos(\omega_f lt) + b_l\sin(\omega_f lt) \tag{12}$$

$$\ddot{q}_i(t) = \omega_f \sum_{l=1}^{N} b_l l\cos(\omega_f lt) - a_l l\sin(\omega_f lt) \tag{13}$$

Assuming the positions, velocities, accelerations and motor torques are measured at a sampling frequency ω_s and the fundamental frequency of the trajectories is ω_f, then a number of $M = \omega_s / \omega_f$ samples can be recorded, and an over-determined equations can be written as:

$$\mathbf{A}\chi_b = \mathbf{b}, \tag{14}$$

where:

$$\mathbf{A} = \begin{bmatrix} \mathbf{Y}(q_1, \dot{q}_1, \ddot{q}_1) \\ \vdots \\ \mathbf{Y}(q_M, \dot{q}_M, \ddot{q}_M) \end{bmatrix}, \quad \mathbf{b} = \begin{bmatrix} \boldsymbol{\tau}_1 \\ \vdots \\ \boldsymbol{\tau}_M \end{bmatrix} \tag{15}$$

The excitation trajectory can be optimized by minimizing the condition number of the observation matrix **A**. The global optimization algorithm DE can be used for this purpose. The trajectory is defined to have zero initial joint positions, velocities and accelerations. And the maximal joint positions, velocities and accelerations are denotes as $q_{\max}$, $\dot{q}_{\max}$, and $\ddot{q}_{\max}$ respectively as seen in the following equations:

$$\min_{a_l, b_l} = cond(\mathbf{A}) \tag{16}$$

subject to

$$\begin{cases} \sum_{l=1}^{N} \frac{b_l}{\omega_f l} = 0, \quad \sum_{l=1}^{N} a_l = 0, \quad \sum_{l=1}^{N} \omega_f l b_l = 0 \\ \sum_{l=1}^{N} \frac{1}{\omega_f l} \sqrt{a_l^2 + b_l^2} \le q_{\max} \\ \sum_{l=1}^{N} \sqrt{a_l^2 + b_l^2} \le \dot{q}_{\max} \\ \omega_f \sum_{l=1}^{N} l \sqrt{a_l^2 + b_l^2} \le \ddot{q}_{\max} \end{cases} \tag{17}$$

After the joint positions, velocities, accelerations and torques are obtained, the base dynamic parameters can be obtained by minimizing a least squares objective function using DE global optimization algorithm.

$$\min_{\chi_b} \|\mathbf{A}\chi_b - \mathbf{b}\|_2^2. \tag{18}$$

where **b** represent the measured torques, and $\mathbf{A}\chi_b$ represent the predicted torques with unknown variables.

4. Simulation and experimental results

To verify the effectiveness of the proposed kinematic and dynamic calibration methods, a six-DOF Mitsubishi RV-3SB manipulator was used. The modified DH parameters are listed in table 1. θ_1 to θ_6 are joint variables whose values are recorded according to joint sensor reading. r_7 is the measured distance from robot end-effector to the tip point on the plane surface, which can be obtained by a high accuracy (at least μm level) range finder or dial indicator. The plane surface has to be put at more than four different locations within the workspace. The plane surface should be very smooth and the flatness should be up to several micrometers. Totally there are 17 parameters can be identified. Most of parameters on the base frame and endpoint frame cannot be identified.

Table 1. The modified DH parameters [6].

Link	α_i	d_i (mm)	θ_i	r_i (mm)	β_i
base	0	0	0	0	0
1	0	0	θ_1	r_1=350	0
2	$-\pi/2+\delta\alpha_2$	$d_2+\delta d_2$	θ_2	$0+\delta r_2$	0
3	$0+\delta\alpha_3$	$d_2+\delta d_3$	θ_3	0	$0+\delta\beta_3$
4	$-\pi/2+\delta\alpha_4$	$d_4+\delta d_4$	θ_4	$r_4+\delta r_4$	0
5	$\pi/2+\delta\alpha_5$	$0+\delta d_5$	θ_5	$r_4+\delta r_5$	0
6	$-\pi/2+\delta\alpha_6$	$0+\delta d_6$	θ_6	$0+\delta r_6$	0
Tip	$0+\delta\alpha_7$	$0+\delta d_7$	0	$85+r_7$	0

Experimental tests are conducted by using a vision-based calibration system to measure the distance r_7 and to record the sensor readings of each joint. Figure 3 shows that the position error of the end-effector is about 1.6 mm before calibration, after calibration, the position error has been reduced to 0.3 mm.

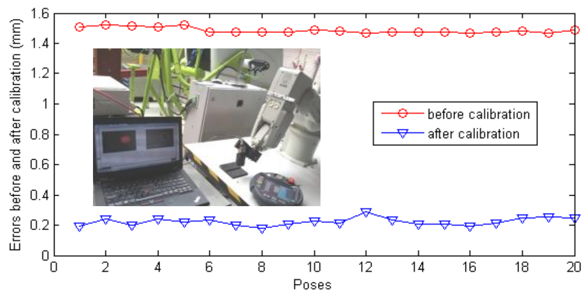

Fig. 3. Experimental calibration results.

To effectively identify the dynamic model parameters, the information of a certain combinations of positions, velocities and accelerations is indispensable. In this work, a Fourier series with five harmonic sine and cosine functions is selected to generate excitation trajectories of positions, velocities and accelerations. By using DE optimization algorithm to the equations (16) and (17), the coefficients of Fourier series can be found and then the optimal joint position trajectories can be obtained as seen in figure 4.

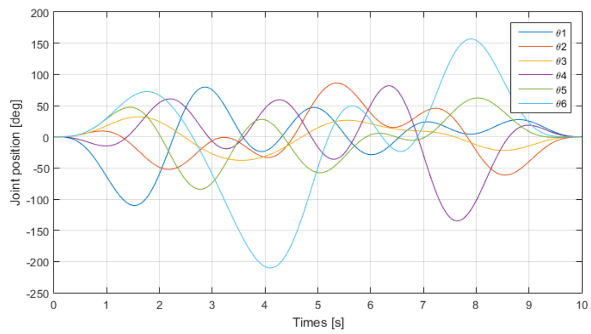

Fig. 4. Joint position excitation trajectories.

After the trajectories of joint positions, velocities and accelerations have been obtained. The next step is to get joint torque values. In practice, the torque value can be acquired via torque sensors or current control. For simulation purpose, this paper utilize SimMechanics to simulate dynamic motions [11]. Figure 5 illustrates a SimMechanics block diagram of the first joint of the RV-3SB robot. The joint input are the excitation trajectories of position, velocity and acceleration, and the output is joint torques. By selecting sampling frequency ω_s as 150 Hz and fundamental frequency ω_f as 0.1 Hz, a total number of 1500 samples per period can be obtained. Substituting these samples into equation (18) for optimization, then the base dynamic parameters can be identified. Figure 6 shows the Cartesian position of the end-effector during the Fourier series trajectory. And figure 7 shows the difference between the estimated torques using identified parameters and the measured torques using SimMechanics. It can be seen the trajectory matches very well with only a little deviations.

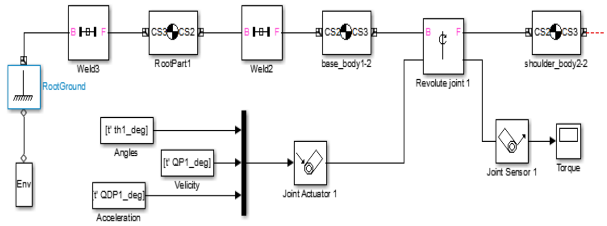

Fig. 5. SimMechanics block diagram for dynamics.

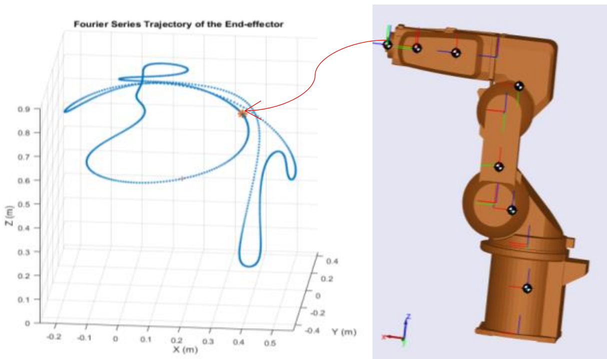

Fig. 6. The end-effector's Cartesian position using Fourier series excitation trajectory approach.

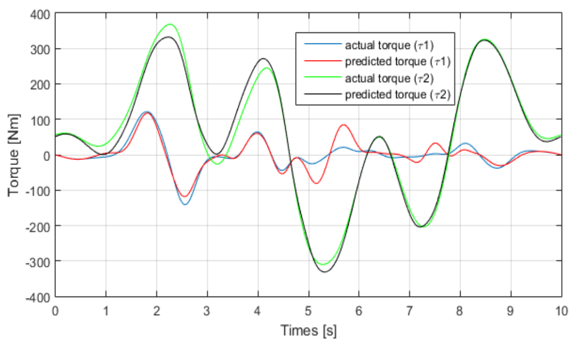

Fig. 7. Estimated torques vs measured torques.

5. Conclusions

In this paper, a plane constraint kinematic calibration method has been investigated. The advantage of this method is that the plane surface can be put in any unknown locations of the manipulator workspace without base calibration in advance. The only thing need to know is to record each joint sensor readings and measure the distance between the robot end-effector and the plane endpoint. This feature makes on-site calibration easy and convenient to implement. This paper has also investigated a SimMechanics simulation based dynamic calibration method. For the remote handling of big size and massive weight component, SimMechanics together with Simulink package in Matlab environment provides an alternative way to verify the effectiveness of dynamic calibration method and its control strategy. The future work will focus on the experimental validation of the proposed dynamic calibration method.

Acknowledgments

This work has been carried out within the framework of the EUROfusion Consortium and has received funding from the Euratom research and training programme 2014-2018 under grant agreement No 633053. The views and opinions expressed herein do not necessarily reflect those of the European Commission.

References

[1] Hollerbach J M., Wampler C W., The calibration index and the role of input noise in robot calibration, Robotics Research. Springer London, (1996): 558-567.

[2] Meggiolaro M A., Scriffignano G, Dubowsky S., Manipulator calibration using a single endpoint contact constraint, Proceedings of ASME Design Engineering Technical Conference, Baltimore, USA. 2000.

[3] Du B., Xi N., Nieves E., Industrial robot calibration using a virtual linear constraint, International Journal on Smart Sensing and Intelligent Systems 5.4 (2012): 987-1000.

[4] Besnard S., Khalil W., Garcia G., Geometric calibration of robots using multiple plane constraints, Advances in robot kinematics. Springer Netherlands, 2000. 61-70.

[5] Wei G Q., Hirzinger G., Active self-calibration of hand-mounted laser range finders, IEEE Transactions on Robotics and Automation, 14(3) (1998): 493-497.

[6] Khalil W, Dombre E. Modeling, identification and control of robots, Butterworth-Heinemann, 2004.

[7] Jin, J., Nicholas G., Parameter identification for industrial robots with a fast and robust trajectory design approach, Robotics and Computer-Integrated Manufacturing 31 (2015): 21-29.

[8] Wang Y., Wu H., Handroos H., Error Modelling and Differential-Evolution-based Parameter Identification Method for Redundant Hybrid Robot, International Journal of Modelling and Simulation, ISSN: 1925-7082, Volume 32 (2012), pp. 255-264.

[9] Gautier M., Briot S., Dynamic parameter identification of a 6 DOF industrial robot using power model, 2013 IEEE International Conference on Robotics and Automation (ICRA). IEEE, (2013): 2914-2920.

[10] Calafiore G., Marina I., Basilio B., Robot dynamic calibration: Optimal excitation trajectories and experimental parameter estimation, Journal of robotic systems, 18.2 (2001): 55-68.

[11] Hage H, Bidaud P, Jardin N, Simulation of a Stäubli TX90 Robot during Milling using SimMechanics, Applied Mechanics and Materials, Trans Tech Publications, (2012) 162: 403-412.